Final Draft
of the original manuscript:

de Queiroz Caetano, G.; Silva, C.C.; Motta, M.F.; Miranda, H.C.; Farias, J.P.; Bergmann, L.A.; dos Santos, J.F.:

Influence of rotation speed and axial force on the friction stir welding of AISI 410S ferritic stainless steel.

In: Journal of Materials Processing Technology. Vol. 262 (2018) 430 - 436.
First published online by Elsevier: July 17, 2018

DOI: 10.1016/j.jmatprotec.2018.07.018
https://dx.doi.org/10.1016/j.jmatprotec.2018.07.018

Influence of Rotation Speed and Axial Force on the Friction Stir Welding of AISI 410S Ferritic Stainless Steel

Author names and affiliations:

Gerbson de Queiroz Caetano[1*], Marcelo Ferreira Motta[1], Hélio Cordeiro Miranda[1], Jesualdo Pereira Farias[1], Cleiton Carvalho Silva[1], Luciano Andrei Bergmann[2], Jorge Fernandez dos Santos[2]

[1] Universidade Federal do Ceará, Department of Materials and Metallurgical Engineering, Campus do Pici, Building 1080, 60440-554 Fortaleza, Ceará, Brazil.

[2]Helmholtz-Zentrum Geesthacht, Institute of Material Research, Material Mechanics, Solid State Joining Processes, Max Planck Strasse 1, 21502 Geesthacht, Schleswig-Holstein, Germany

*Corresponding author.

Phone: +55 85 33669358

Fax: +55 85 33669969

E-mail: gerbsonqueiroz@gmail.com

Abstract. This work aimed to investigate a ferritic stainless steel AISI 410S weldedby friction stir welding (FSW), evaluating the rotation speed and axial force in order to be able to producejoints without defects. The parameter variation has been selected in order to provided a combination of acceptable surface finish, absence of cracks, and full tool penetration. In this worksix welds has been performed, varying the rotation speed between two levels and the axial force from 10 to 30 kN,keeping the welding speed constant at 1 mm/s. Through the analysis of the process parameters it was possible to verify that the torque exerted by the tool decreased with the decrease of the axial force, the rotational speed had the main contribution onthe heat input. Instability in the application of the axial force directly implies the formation of volumetric defects along the stir zone. Thus, it was possible to establish an optimum combination of parameters for the FSW process in order to ensure successful welding of the AISI 410S steel, resulting in welds without internal defects and with good surface finish.

Key-words: Stainless Steel (A), welding (C).

1. INTRODUCTION

Among the stainless steels, the ferritic family is characterized by having a substantially ferritic microstructure at room temperature and thus having a body centered cubic (BCC) crystalline structure. Its chromium content may range from 11 to 30% and it may also contain additions of Mo, Nb, Ti, and others. Compared to austenitic stainless steels, which are the most frequently used commercially because of their good corrosion and mechanical strength, ferritics provide approximately the same corrosion resistance but have lower ductility, toughness, and weldability (Smith, 1993). However, ferritic stainless steels can be used in a wide variety of applications where resistance against pitting corrosion and/or stress corrosion cracking is more important than mechanical strength (Kotecki and Lippold, 2005). Another great advantage of ferritic stainless steels is the reduction or absence of nickel in their composition, since nickel is one of the most expensive alloying elements and thus considerably increases the price of austenitic stainless steels compared to ferritic stainless steels (Silva et al., 2007).

A large gap to be filled in relation to the expansion of the applications of the ferritic stainless steels is regarding to the metallurgical problems resulting from the fusion welding of these steels. The thermal cycles to which these materials are submitted cause metallurgical problems, compromising their weldability. Among the main deleterious effects that welding can cause in these steels, we can highlight the grain growth, which causes a decrease in the toughness and compromises the mechanical resistance (Silva et al., 2007). Another problem is the precipitation of chromium, nitrides, and carbides, which cause embrittlement and intergranular corrosion. In addition, the formation of embrittlement phases such as σ-phase and χ-phase can also have a detrimental effect on the mechanical and corrosion resistance of the material (Machado et al., 2006; Silva et al., 2008).

In recent decades, friction stir welding (FSW), a solid-state welding process developed by The Welding Institute (TWI) of Cambridge in England, has revolutionized the joining of materials that were considered not weldable or difficult to be welded. This process uses a non-consumable tool that rotates and translates the workpiece, resulting in heating and

plastic deformation of the material to be joined. In this case, the material is heated at temperatures below those experienced in fusion welding (Mishra and Ma, 2005).

Among the advantages commonly attributed to the FSW process are the good strength and ductility of the welds with minimal residual stress and distortion, absence of defects related to melting of the material, smaller heat affected zone, and a grain refined microstructure that increases the tensile strength and fatigue life (Bilgin and Meran, 2012; Cavaliere et al., 2006; Sathiya et al., 2006). In this process, the rotational speed and the axial force are the parameters that are directly related to the generation of heat, reducing the rotational speed, decrease the temperature during the process. A combination of welding speed, axial force and Rotational Speed that give the key factor for process optimization. Thus, the correct adjustment of these parameters allows the joining of metals, especially those that present difficult weldability when traditional fusion processes are applied (Silva et al., 2008). In the case of ferritic stainless steels, a low heat input and high welding speed are recommended to avoid ferritic grain growth and to form a refined microstructure. However, such characteristics can be achieved very well by using the FSW process (Bilgin and Meran, 2012). Therefore, this work aims to analyse the effect of the welding parameters of AISI 410S ferritic stainless steel in the FSW process, evaluating operational and metallurgical aspects for the production of joints without defects.

2. MATERIALS AND METHODS

The welds were made using 4-mm-thick plates of AISI 410S ferritic stainless steel. The chemical composition of the material was determined by optical emission spectroscopy and is presented in Table 1.

The joining of samples by the FSW process in this study was carried out at the Helmholtz-Zentrum Geesthacht (HZG) in Germany. All welds were made using the HZG Gantry System. An inert gas injection system (Ar) was used to protect the material during the process, since at temperatures above 535 °C, this stainless steel tends to react with the atmosphere. It also has an integrated system to record the Process data, like (Plunge depth, Rotational Speed, torque, Forces Applied to the tool and tool position over time).

For the butt joints a polycrystalline cubic boron nitride (PCBN) tool were used, as shown in Fig. 1. The tool had a conical diameter of 23 or 25 mm with a conical pin with a diameter of 9.2 mm and a length of 3.7 mm. The pin had a conical surface with the

presence of negative recesses, which were in the form of a spiral with respect to the axis of symmetry of the tool.

The metal flow in FSW is composed of two modes of transfer, occurring due to either the extrusion of metal around the tool probe or the frictional heat generated between the tool shoulder and the sample (Muthukumaran and Mukherjee, 2006). As the intensity of the frictional contact between the tool shoulder and the workpiece is one of the main factors responsible for the elimination of defects, parameters such as axial force and rotation speed directly affect this transfer mode (Sinha et al., 2008). In this work, six welding conditions were tested to evaluate the interfluence of the process parameters in the heat generation and defect formation. Thus, the rotational speed was varied between 450 rpm and 800 rpm, with axial forces changing from 10 to 30 kN. For both rotational speeds used, the tool tilt angle was maintained at 0º and the welding speed was 1 mm/s.

These parameters were related to the energy of the process and the heat input generated during the FSW process was calculated by Equation 1 according to a study by Deqing et al. (2004):

$$\boldsymbol{E = \pi \,.\, \mu \,.\, Ps \,.\, VR \,.\, \frac{D^2 + D\,.d + d^2}{45\,.(D+d)}} \qquad \text{(Eq.I)}$$

where E is the heat input (J/m), μ is the friction coefficient of the material, Ps is the pressure exerted by the support on the material (Pa), VR is the speed of rotation (rad/s), D is the diameter of the shoulder, and d is the diameter of the pin (m).

For macroscopic analysis, the welds were initially cut by means of a diamond abrasive disc in a Struers Discotom-6 cutter. For grinding, sandpapers with granulometry between 120 and 2500 mesh were used. The polishing step was performed in a Buehler Phoenix 4000 universal polisher with diamond pastes of 3, 1, and 1/4 μ at a rotation speed of 150 rpm, and subsequently electrolytic etching was performed with 40% nitric acid using a voltage of 3 V for 2 minutes for analysis by optical microscopy using a Carl Zeiss optical microscope integrated with AxioVision SE64 software.

3. RESULTS AND DISCUSSIONS

3.1 Rotation Speed

The process parameters interfere directly in the heat input, which strongly influences the heating and cooling rates of the thermal cycle and consequently the resultant microstructure. However, the energy calculated based on the process parameters corresponds to an equivalent energy and not exactly to the energy produced during the process, since there are losses that were not considered, the main ones being conduction and convection in the region of the weld.

The rotation speed is the parameter related to the frictional force and friction at the interface between the material and the tool and is therefore directly linked to the heat generation during the welding process (Bilgin and Meran, 2012; Lakshminarayanan and Balasubramanian, 2013). The frictional coupling of the tool surface with the joint governs the heating mechanism and the rotation of the tool results in agitation and mixing of the material around the probe. Thus, the higher the rotational speed, the higher will be the temperature in the process, due to the increase of the friction heating (Colegrove et al., 2007; Mishra and Ma, 2005; Uday et al., 2010).

Among the welds of AISI 410S ferritic stainless steel produced by FSW, it is possible to observe the strong influence of the rotation speed on the heat generation, since the reduction in rotation speed from 800 to 450 rpm between Conditions 3 and 4, in which welding was performed with an axial force of around 20 kN, generated a drop in heat input of around 400 J/mm, as can be observed in Fig. 2.

3.2 Axial Force

Analyzing the axial force, it is possible to observe that the instability in its application results in a lack of forging required to guarantee the consolidation of the joint and consequently leads to the formation of volumetric defects (Kim et al., 2006). The instabilities observed under Conditions 5 and 6 directly reflect the poor quality of these welds, a fact not observed under Condition 4 (Fig. 3). It is possible to infer that the increase of the force also provided a higher amount of heat in the process, which was responsible for raising the temperature and for the degree of softening of the material, even with less influence as the rotation speed, the heat input decreases as the force decreases.

It can be observed that the six curves of axial force over time initially exhibited a similar behavior. During the initial phase of the process, a pressure gradient emerged along the penetration channel. The increase of the pressure was counterbalanced by the

increase of the axial force. After the tool reached the desired depth of penetration, the pressure gradient decreased until it reached a steady state. After reaching equilibrium, new abrupt changes in the curve of axial force × time characterize a nonuniformity of force application, compromising the flow of the material and resulting in the formation of defects.

By analysing the parameters of the FSW process, it is also possible to observe that the torque exerted by the tool increases with the increase of the axial force. For the FSW joints of the AISI 410S ferritic stainless steel on evaluating the torque under Condition 1, in which 30 kN of force was applied, which is higher than force of 22 kN applied under Condition 3, it can be observed that the greater the force, the greater the pressure of the tool on the material, as a greater torque is necessary for the consolidation of the rotation of the tool, as shown in Fig. 4 (Buchibabu et al., 2017). [17]. The rotation speed also causes changes in the torque due to the greater or lesser degree of plasticity of the metal caused by the changes of heat input, and therefore both the rotation speed and the applied axial force are determinant factors in the evolution of the torque during the FSW process, which is in agreement the report by Leitão et al. (2012).

3.3 Surface Finish

Analysing the surface of the AISI 410S steel welded by FSW, it is possible to observe that under the welding conditions with a rotation speed of 800 rpm, the flash is directly related to the increase of the axial force, which causes an increase in the heat input. As noted by Trueba et al. (2015), higher welding temperatures in FSW provide greater ease of metal flow and the displacement of a greater amount of material by the tool probe, which makes it more difficult for the shoulder to restrain the displaced metal and causes flash formation. Observing Fig. 5 in detail, it is verified that the amount of flash decreases as the axial force decreases from 30 to 22 kN, and these flashes are more critical in the samples joined under Condition 1, which involves higher axial force.

In the conditions in which weld was performed with a rotational speed of 450 rpm, the presence of flash was checked under the conditions with the smallest forces, which can be analysed under Conditions 5 and 6 in which axial forces of 15 and 10 kN, respectively, were applied (Fig. 5). This occurred due to the instability of the axial force, which caused irregularities in the stir zone and consequent material losses. According to the analysis of defects in FSW welds performed by Threadgill (2007), the production of

flash can occur due to both high heat input and irregularities in the application of the axial force, generating an inadequate material flow with the formation of voids and loss of plastified material.

In none of the conditions evaluated in this work,could be observed any surface defect or superficial cavity. These defects are associated to a lack of heat or excess of heat in the material during welding process, which indicates that even under the conditions with the lowest rotation speed and, consequently, lower heat input, the heat generated in the region near the tool shoulder was sufficient to confer on the material a good viscosity and plasticity, which was not observed in most internal regions close to the tool probe.

3.4 Defect Analysis

Based on the cross-section analysis of the FSW joints of the AISI 410S ferritic stainless steel, it was possible to verify the consolidation of FSW joints and absence of defects under both rotational speeds, 800 and 450 rpm. The material flow reached an adequate state of plastification due to the heat intensity obtained by the combination of the used parameters, as also observed by Kim et al. (2016) in FSW of 430M2 ferritic stainless steel using a rotational speed of 900 rpm.

However, by macroscopic analysis of the cross-section of the FSW samples analysed, it is possible to verify voids under Conditions 5 and 6, where samples were welded with a rotation speed of 450 rpm and axial forces of 15 kN and 10 kN, respectively. This behavior was attributed to a lower interaction between the tool and the material, due to the low axial force and as consequence reduced friction force and necessary heat to achieve an adequate plasticizing state of the material to flow during the FSW process (Fig. 6) (Tongne et al., 2015). According Doude et al. (2015), these voids in the stir zone in regions close to the root of the weld, as observed in Condition 5, refer to the use of parameters whose values are below the optimum recommended for consolidation of a defect-free FSW joint, due to the use of a low rotation speed and low axial force.

Evaluating the cross-sectional macrographs of the FSW welds, it is possible to reaffirm the high flash was formed under Condition 1, in which a rotation speed of 800 rpm and axial force of 30 kN were applied, as previously showed in the analysis of the surface finish presented in Fig. 5. As the axial force decreases to 25 and 22 kN, a decrease in flash occurs, as can be observed in Fig. 7.

In Condition 1, it is also possible to observe excess penetration due to the high force that has been applied. However, as the axial force and rotation speed decrease, root flaws occurs. This particular weld defect can be observed in Fig. 8 and is associated with the insufficient penetration of the tool (Edwards and Ramulu, 2015) Thus, this demonstrates that the production of AISI 410S ferritic stainless steel joints by the FSW process without root flaws should be carried out with not only an increase or decrease of the axial force, but also with a balance between axial force and angle of the tool, enabling a greater immersion of the tool probe into the joint, as stated by Shultz et al. (2010). Besides, the correct balance between tool angle and axial force in FSW joints without root flaw defects can also be obtained with the correct balance between axial force and rotation speed without the need to vary the angle of the tool, as can be verified in this study.

Under the conditions in which a rotation speed of 450 rpm was applied, the macroscopic analysis confirmed interferences in the application of axial force, revealing the presence of wormholes throughout the stir region, which is more critical for Condition 6, in which an axial force of 10 kN was used. (Fig. 9). This lack of filling or tunnel defect consists of internal regions of the welded joint with the absence of material, forming voids along the length of the weld. According Mishra and Ma (2005), this is caused by the lack of heating of the material by the cold parameters, such as low rotational speeds and low axial forces, which generate less friction or less time of permanence of the tool on the material. Kumar and Kailas (2008) claim that in addition to low heating, the lack of shoulder pressure on the material also affects the flow, preventing it from filling the entire weld region.

Therefore, FSW joints of AISI 410S ferritic stainless steel with satisfactory surface finish and no defects in the stir zone can be obtained using parameters that ensure adequate heat intensity to plasticize the material flow, which can be obtained by increasing the axial force to 800 rpm; however, increasing the axial force to values higher than 25 kN is not adequate, because as well as accentuating the production of flash it can lead to the formation of flaws in the root of the joint due to excess penetration.

4. CONCLUSIONS

Based on the experimental results concerning the analysis of the parameters of the FSW process and its implications in the formation of defects for the welding of the AISI 410S ferritic stainless steel, it was possible to conclude that:

1. With the appropriate combination of welding parameters it was possible to weld the AISI 410S ferritic stainless steel successfully, producing a stable joint without defects.
2. Instability in the process leads to vibration and consequently a lack of forging of the material (that is visible in the force graphic) during the movement of the tool to ensure consolidation of the joint and consequently results in the formation of volumetric defects along the stir zone.
3. The torque exerted by the tool decreases with the decrease in the force applied, because the smaller friction applied by rotation and force, the lower the tool pressure on the material and the less torque is required to consolidate the tool rotation.
4. The production of flash can occur because of the increase in axial force, as this increases the heat input and allows the formation of a larger amount of plastified material, and because of the instability of the application of axial force.
5. The production of joints in AISI 410S ferritic stainless steel welded by the FSW process without root flaws is achieved through a balance between the force and the correct balance between the axial force and rotation speed, which allows a greater immersion of the tool probe in the joint.
6. The best combinations of FSW parameters for the production of welded joints without defects were the combination of a rotation speed of 450 rpm with an axial force of 20 kN and a rotation speed of 800 rpm with an axial force of 22 kN. In both cases, the welding speed was maintained at 1 mm/s.

5. ACKNOWLEDGMENTS

The authors would like to thank the Laboratório de Pesquisa e Tecnologia em Soldagem (LPTS) and the Helmholtz-Zentrum Geesthacht (HZG) as well as CNPq and FUNCAP for funding the project and the Department of Metallurgical and Materials Engineering of the Federal University of Ceará for the master's degree.

6. REFERENCES

Bilgin, M.B., Meran, C., 2012. The effect of tool rotational and traverse speed on friction stir weldability of AISI 430 ferritic stainless steels. Mater. Des. 33, 376–383.

Buchibabu, V., Reddy, G.M., De, A., 2017. Probing torque, traverse force and tool durability in friction stir welding of aluminum alloys. J. Mater. Process. Technol. 241, 86–92.

Cavaliere, P., Campanile, G., Panella, F., Squillace, A., 2006. Effect of welding parameters on mechanical and microstructural properties of AA6056 joints produced by friction stir welding. J. Mater. Process. Technol. 180, 263–270.

Colegrove, P.A., Shercliff, H.R., Zettler, R., 2007. Model for predicting heat generation and temperature in friction stir welding from the material properties. Sci. Technol. Weld. Join. 12, 284–297.

Deqing, W., Shuhua, L., Zhaoxia, C., 2004. Study of friction stir welding of aluminum. J. Mater. Sci. 39, 1689–1693.

Doude, H., Schneider, J., Patton, B., Stafford, S., Waters, T., Varner, C., 2015. Optimizing weld quality of a friction stir welded aluminum alloy. J. Mater. Process. Technol. 222, 188–196.

Edwards, P.D., Ramulu, M., 2015. Material flow during friction stir welding of Ti-6Al-4V. J. Mater. Process. Technol. 218, 107–115.

Kim, K.H., Bang, H.S., Kaplan, A.F.H., 2016. Joint properties of ultra thin 430M2 ferritic stainless steel sheets by friction stir welding using pinless tool. J. Mater. Process. Technol.

Kim, Y.G., Fujii, H., Tsumura, T., Komazaki, T., Nakata, K., 2006. Three defect types in friction stir welding of aluminum die casting alloy. Mater. Sci. Eng. A 415, 250–254.

Kotecki, D. J, Lippold, J.C., 2005. Welding metallurgy and weldability of stainless steels. John Wiley & Sons, New Jersey, USA.

Kumar, K., Kailas, S.V., 2008. The role of friction stir welding tool on material flow and weld formation. Mater. Sci. Eng. A 485, 367–374.

Lakshminarayanan, A.K., Balasubramanian, V., 2013. Process Parameters Optimisation for Friction Stir Welding of AISI 409M Grade Ferritic Stainless Steel. Exp. Tech. 37, 59–73.

Leitao, C., Louro, R., Rodrigues, D.M., 2012. Using torque sensitivity analysis in accessing Friction Stir Welding/Processing conditions. J. Mater. Process. Technol. 212, 2051–2057.

Machado, J.P.S.E., Silva, C.C., Sobral-Santiago, A.V.C., Sant'Ana, H.B. de, Farias, J.P., 2006. Effect of temperature on the level of corrosion caused by heavy petroleum on AISI 304 and AISI 444 stainless steel. Mater. Res. 9, 137–142.

Mishra, R.S., Ma Z.Y., 2005. Friction stir welding and processing, Mater. Sci. Eng. R Rep. 50, 1–78.

Muthukumaran, S., Mukherjee, S.K., 2006. Two modes of metal flow phenomenon in friction stir welding process. Sci. Technol. Weld. Join. 11, 337–340.

Sathiya, P., Aravindan, S., Haq, A.N., 2006. Effect of friction welding parameters on mechanical and metallurgical properties of ferritic stainless steel. Int. J. Adv. Manuf. Technol. 31, 1076–1082.

Shultz, E.F., Cole, E.G., Smith, C.B., Zinn, M.R., Ferrier, N.J., Pfefferkorn, F.E., 2010. Effect of compliance and travel angle on friction stir welding with gaps. J. Manuf. Sci. Eng. 132, 41010.

Silva, C.C., Farias, J.P., Miranda, H.C., Guimarães, R.F., Menezes, J.W.A., Neto, M.A.M., 2008. Microstructural characterization of the HAZ in AISI 444 ferritic stainless steel welds. Mater. Charact. 59, 528–533.

Silva, C.C., Machado, J.P.S.E., Sobral-Santiago, A.V.C., de Sant'Ana, H.B., Farias, J.P., 2007. High-temperature hydrogen sulfide corrosion on the heat-affected zone of the AISI 444 stainless steel caused by Venezuelan heavy petroleum. J. Pet. Sci. Eng. 59, 219–225.

Sinha, P., Muthukumaran, S., Mukherjee, S.K., 2008. Analysis of first mode of metal transfer in friction stir welded plates by image processing technique. J. Mater. Process. Technol. 197, 17–21.

Smith, W. F., 1993. Structure and Properties of Engineering Alloys, 2nd edition. ed. McGraw-Hill (New York).

Threadgill, P.L., 2007. Terminology in friction stir welding. Sci. Technol. Weld. Join. 12, 357–360.

Tongne, A., Jahazi, M., Feulvarch, E., Desrayaud, C., 2015. Banded structures in friction stir welded Al alloys. J. Mater. Process. Technol. 221, 269–278.

Trueba, L., Heredia, G., Rybicki, D., Johannes, L.B., 2015. Effect of tool shoulder features on defects and tensile properties of friction stir welded aluminum 6061-T6. J. Mater. Process. Technol. 219, 271–277.

Uday, M.B., Ahmad Fauzi, M.N., Zuhailawati, H., Ismail, A.B., 2010. Advances in friction welding process: a review. Sci. Technol. Weld. Join. 15, 534–558.

List of Figure Captions

Figure 1 - Configuration of AISI 410S steel joints and PCBN-based tool used at work.

Figure 2 - Equivalent heat input calculated for the different welding conditions applied to AISI 410S steel by the FSW process.

Figure 3 - Variation of the axial force during welding by the FSW process for AISI 410S steel.

Figure 4 - Variation of the torque throughout the FSW process for AISI 410S steel.

Figure 5 - Surface finishing of different FSW welds produced for AISI 410S steel as a function of the rotation speed and axial force applied.

Figure 6 - Cross-sectional macrographs of different welded conditions of AISI 410S steel.

Figure 7 - (A) Flash Excess in Condition 1. (b) Flash Decrease in Condition 3. (50x).

Figure 8 - (a) Root Flaws due to the excess penetration in Condition 1. (b) Root Flaws due to lack of penetration in Condition 2 (50x).

Figure 9 - (a) Worm hole in condition 5. (b) Voids and Worm hole in condition 6. (50x).

Tables

Table 1- Chemical composition of the material (% weight).

Material	Elements											
	C	Si	Mn	P	S	Cr	Ni	Mo	Cu	Co	N	Fe
410S	0,025	0,37	0,30	0,023	<0,010	12,8	0,21	0,01	0,21	0,02	0,033	Bal.

Table 2 - Welding Parameters AISI 410S

Condition	Rotation Speed (rpm)	Axial Force (kN)
1	800	30
2	800	25
3	800	22
4	450	20
5	450	15
6	450	10

Figure 1

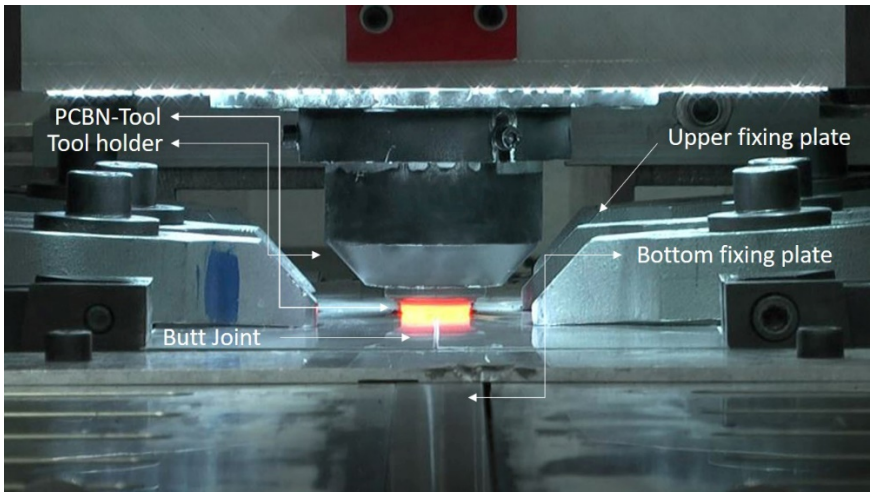

Figure 2

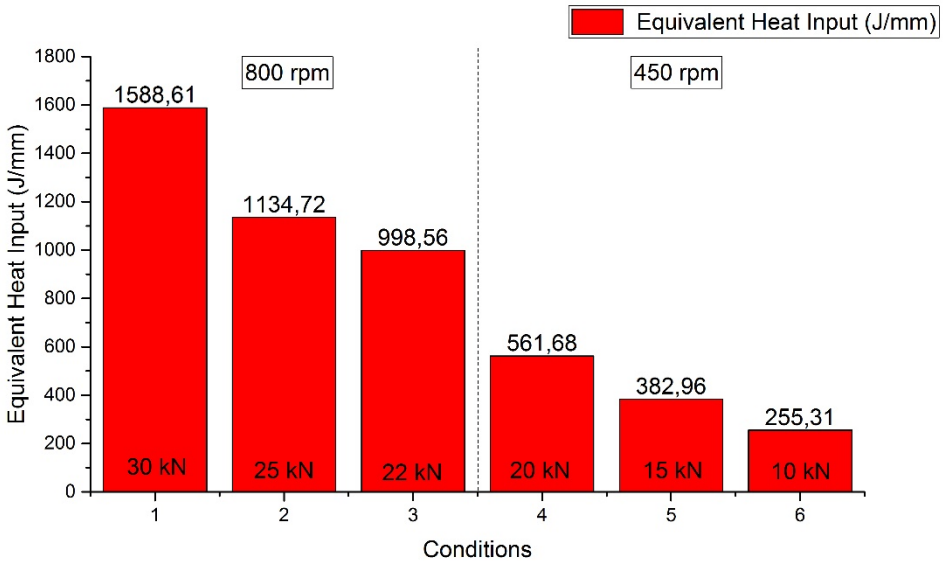

Figure 3

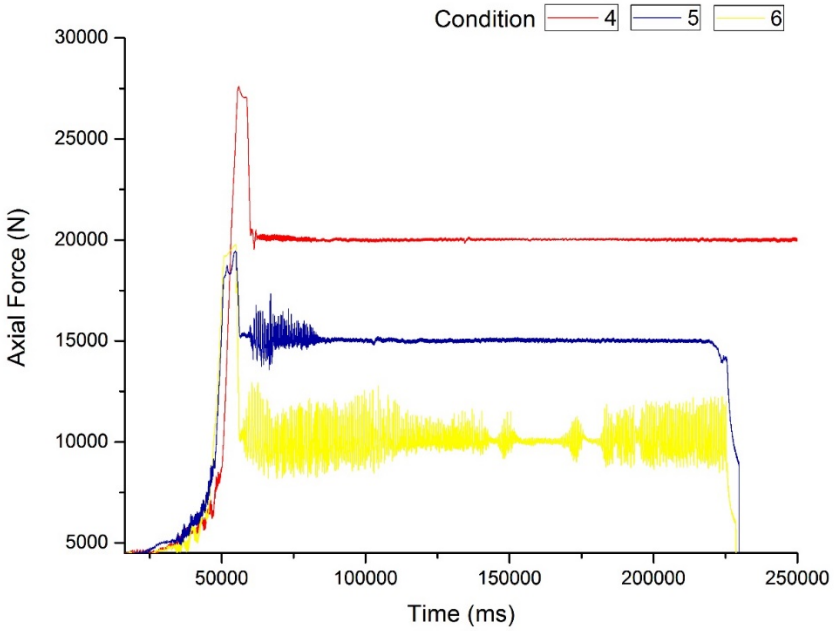

Figure 4

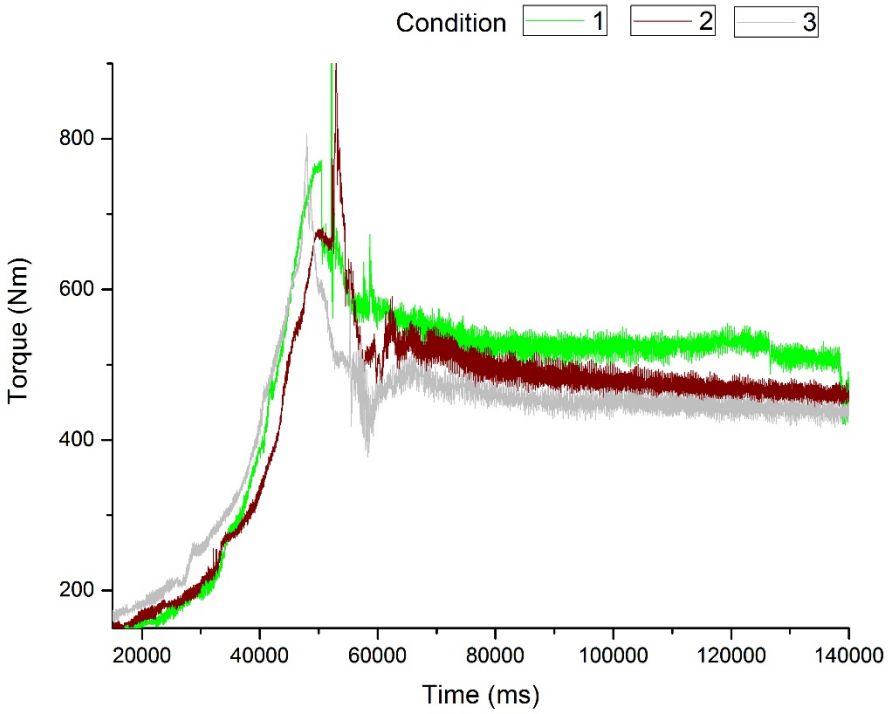

Figure 5

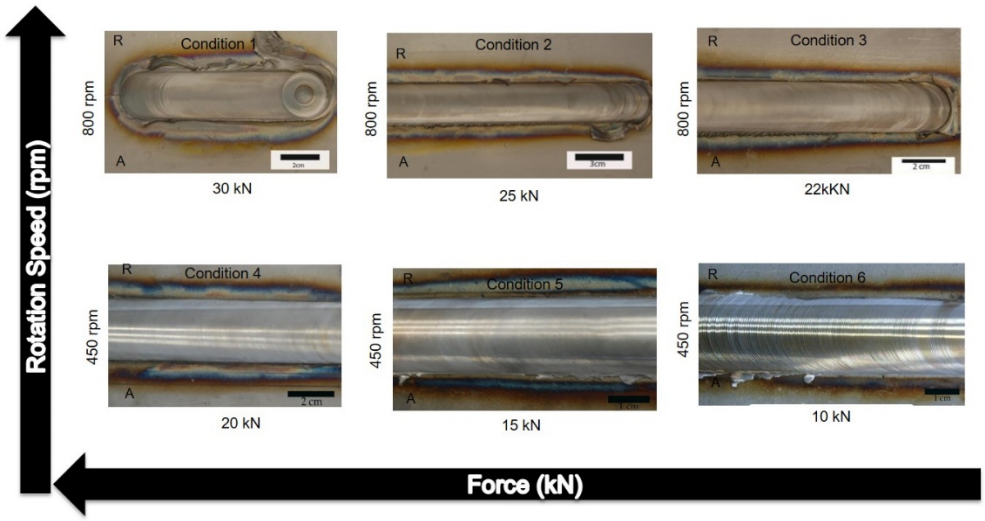

Figure 6

	**<u>Condition 1</u>** 800 RPM 30 KN
	**<u>Condition 2</u>** 800 RPM 25 KN
	**<u>Condition 3</u>** 800 RPM 22 KN
	**<u>Condition 4</u>** 450 RPM 20 KN
	**<u>Condition 5</u>** 450 RPM 15 KN
	**<u>Condition 6</u>** 450 RPM 10 KN

Figure 7

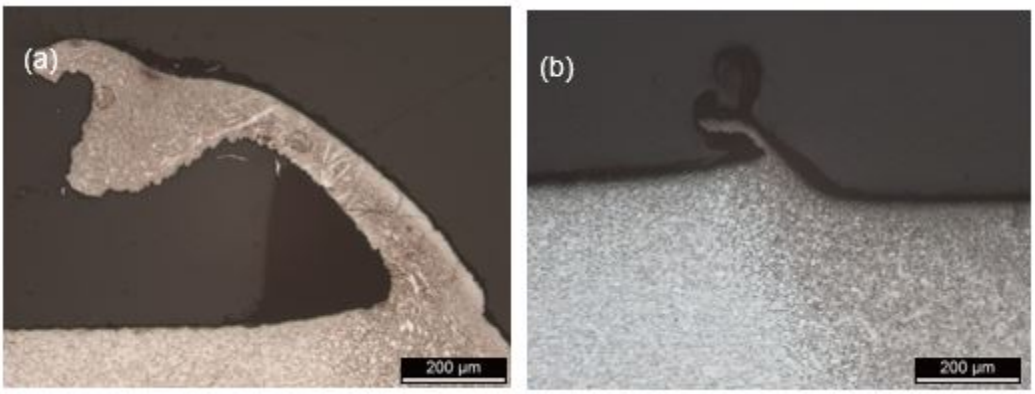

Figure 8

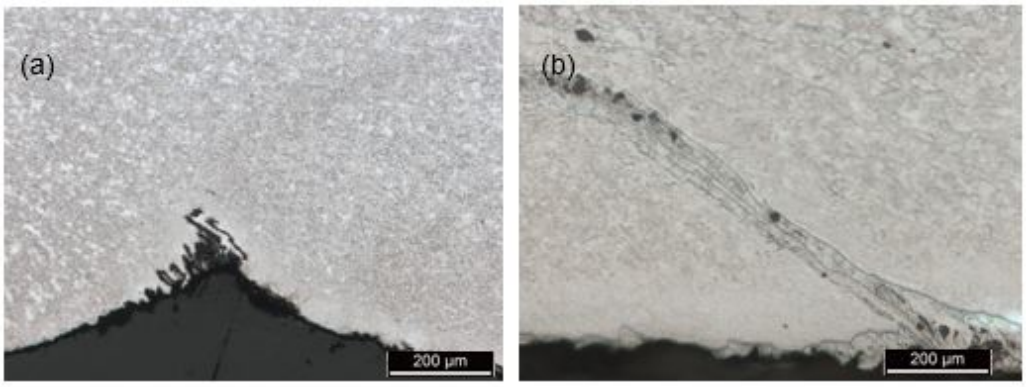

Figure 9